



Direct observation of the nuclear motion during ultrafast intramolecular proton transfer

S. Lochbrunner*, K. Stock, E. Riedle

Lehrstuhl für BioMolekulare Optik, Sektion Physik, Ludwig-Maximilians-Universität, Oettingenstrasse 67, 80538 München, Germany

Received 24 November 2003; revised 27 January 2004; accepted 29 January 2004

Abstract

The skeletal motions contributing to the reaction path of the ultrafast excited state intramolecular proton transfer (ESIPT) are determined directly from time resolved measurements. We investigate the ESIPT in the compounds 2-(2'-hydroxyphenyl)benzothiazole, 2-(2'-hydroxyphenyl)benzoxazole and *ortho*-hydroxybenzaldehyde by UV–visible pump-probe spectroscopy with 30 fs resolution. The proton transfer is observed in real time and a characteristic ‘ringing’ of the molecule in a small number of vibrational modes is found after the reaction. The results show that a bending motion of the molecular skeleton reduces the proton donor–acceptor distance and an electronic configuration change occurs at a sufficient contraction leading to the bonds of the product conformer. The process evolves as a ballistic wavepacket propagation on an adiabatic potential energy surface. The proton is shifted by the skeletal motions from the donor to the acceptor site and tunneling has not to be considered.

© 2004 Elsevier B.V. All rights reserved.

Keywords: Excited state intramolecular proton transfer; Hydrogen dynamics; Ultrafast spectroscopy; Wavepacket motion; Vibrations

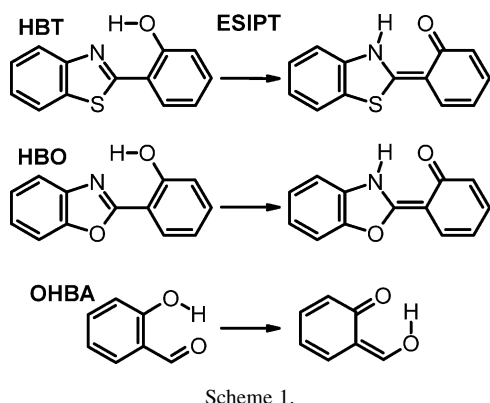
1. Introduction

The dynamics of hydrogen bonds and the reactive proton transfer (PT) are intimately connected with the stability, functionality and conformational dynamics of biomolecules as well as the acidic or basic behavior of many compounds [1]. Much work has been undertaken to characterize these processes and the associated potential energy surfaces (PESs) and to unravel the underlying mechanisms. Steady state spectroscopy has been very successfully applied to find and characterize the vibronic eigenstates involved in these processes [2–4]. Because these states sample large areas of the PESs, the obtained results are very challenging to analysis especially with respect to the dynamics.

Experiments with extremely high time resolution represent a direct and complementary access to the dynamics [5]. They are able to observe the changes and motions on the molecular level in real time. For this purpose, it is necessary to start the process at an exactly defined time. This is possible in excited state intramolecular

proton transfer (ESIPT). Molecules exhibiting ESIPT typically contain an H-chelate ring with an intramolecular hydrogen bond. In the ground state, they adopt the enol form in which the hydrogen is bound to an oxygen atom. In the first electronically excited state, the keto form with the hydrogen transferred to a nitrogen or second oxygen atom at the other side of the ring is the more stable form [6]. After optical excitation of the enol form ESIPT takes place and the keto form is generated. Scheme 1 shows the process for the compounds 2-(2'-hydroxyphenyl)benzothiazole (HBT), 2-(2'-hydroxyphenyl)benzoxazole (HBO) and *ortho*-hydroxybenzaldehyde (OHBA) that are investigated in this study. The ESIPT leads to a large Stokes shift between the fluorescence and the absorption spectrum [6] that has been reported for the compounds under investigation (HBT: Refs. [7,8]; HBO: Ref. [9]; OHBA: Ref. [10]). In our experiments, the ESIPT is initiated by an ultrashort light pulse that promotes all the molecules investigated simultaneously from the ground state to the electronically excited state. Due to the intramolecular character and the ring stabilizing hydrogen bond, the starting geometry is fixed and the dynamics and mechanism of PT are studied under well defined conditions.

* Corresponding author. Tel.: +49-8921809254; fax: +49-8921809202.
E-mail address: stefan.lochbrunner@physik.uni-muenchen.de (S. Lochbrunner).



Previous pump-probe experiments demonstrated that the ESIPT is very fast [7,11] and proceeds even on a sub-100 fs time-scale [9,12]. Measurements with an improved time resolution on 2-(2'-hydroxy-5'-methylphenyl)benzotriazole (TINUVIN P) showed for the first time that skeletal vibrational modes are coherently excited after the process [13].

We investigated the ESIPT of several compounds by transient absorption spectroscopy with a time resolution of 30 fs and observed the nuclear motions during this process [10,14,15]. The transient absorption signals exhibit the characteristic features of vibrational wavepacket dynamics. The vibrational modes of the molecular skeleton contributing to the reaction path are identified from the oscillatory signal components. We performed this analysis for HBT [8,15] and OHBA [10] (see Scheme 1). Here, we give a comparison of the results and include in the analysis new data on HBO. The common features of the nuclear motions during the PT are elaborated giving insight in the course of the reaction path. We discuss the interplay between the electronic and nuclear degrees of freedom and demonstrate that the proton itself plays a rather passive role.

2. Experimental

The transient absorption measurements were performed with a pump-probe spectrometer based on two non-collinearly phase matched optical parametric amplifiers (NOPAs) [14,16]. The NOPAs are pumped by a home built Ti:sapphire laser delivering approximately 100 fs long NIR pulses at around 800 nm with a repetition rate of 1 kHz. The NOPAs provide pulses tunable throughout the visible spectral region that are compressed by a fused silica prism sequence to below 20 fs. The output of one NOPA is frequency doubled in a nominally 100 μm thick BBO crystal cut for type I phase matching and the dispersion of the resulting UV pulses is compensated with a second fused silica prism sequence. The UV pulses are guided to a motorized delay stage and then focused onto the sample to a spot size of 200 μm . The output of the second NOPA is used as probe beam. It is focused to a size of 80 μm at the sample

and crosses the pump beam with a small angle of 3° . The sample transmission is measured by detecting the energy of the probe pulses with a photodiode behind the sample. To account for small variations of the probe beam, a reference beam is split off before the sample and measured with a second photodiode. The sample is a 70 μm thick free flowing liquid jet or a flow cell with a channel thickness of 120 μm . In both cases, the excited volume of the sample solution is replaced by a fresh one between successive laser shots. The ESIPT molecules are dissolved in cyclohexane with a concentration of 10^{-2} – 10^{-3} M resulting in an absorption of about 50% of the pump light.

3. Results and discussion

3.1. Wavepacket dynamics of ESIPT

Fig. 1 shows the transient transmission after photoexcitation of HBT (347 nm excitation wavelength) and HBO (340 nm) at probe wavelengths in the blue and red wing of the keto emission spectra. All traces show an increase of the transmission with a delay of several 10 fs and characteristic oscillations. The Fourier transforms of the oscillatory contributions are depicted in the insets of Fig. 1. The transmission increase is due to the onset of the keto emission. Bleaching of the enol form does not contribute because the enol absorption is in the UV and well separated from the probed spectral region. We can therefore be absolutely sure that the observed kinetics are due to the dynamics of the molecule in the excited electronic state. The signal oscillations are caused by the coherent excitation of specific vibrational modes in the keto form as a result of the ESIPT. The coherently excited modes lead to oscillatory shifts of the emission spectrum that are detected as transmission changes at the fixed probe wavelength [8,17]. The transmission decrease at time zero is caused by the excited state absorption (ESA) from the S_1 state to higher electronic states. The ESA leads to an increased absorption immediately when the pump pulse has promoted the molecule to the S_1 state.

In the case of OHBA, the transient absorption behaves in a similar way (see Fig. 2). A transmission increase due to the rise of the product emission is observed shortly after an initial decrease due to the onset of ESA at delay time zero. Subsequent oscillatory contributions with characteristic frequencies are found that are damped on a picosecond time-scale.

For a quantitative analysis, a model function is fitted to the time resolved data (solid lines in Fig. 1 and Fig. 2) [8]. The transmission increase is modeled with a delayed step-like emission rise. The values of the fitted delays are given for the presented measurements in Table 1. To account for the ESA, the function contains a step-like transmission decrease at time zero. Both step-like contributions are convoluted with the cross-correlation. The oscillatory signal

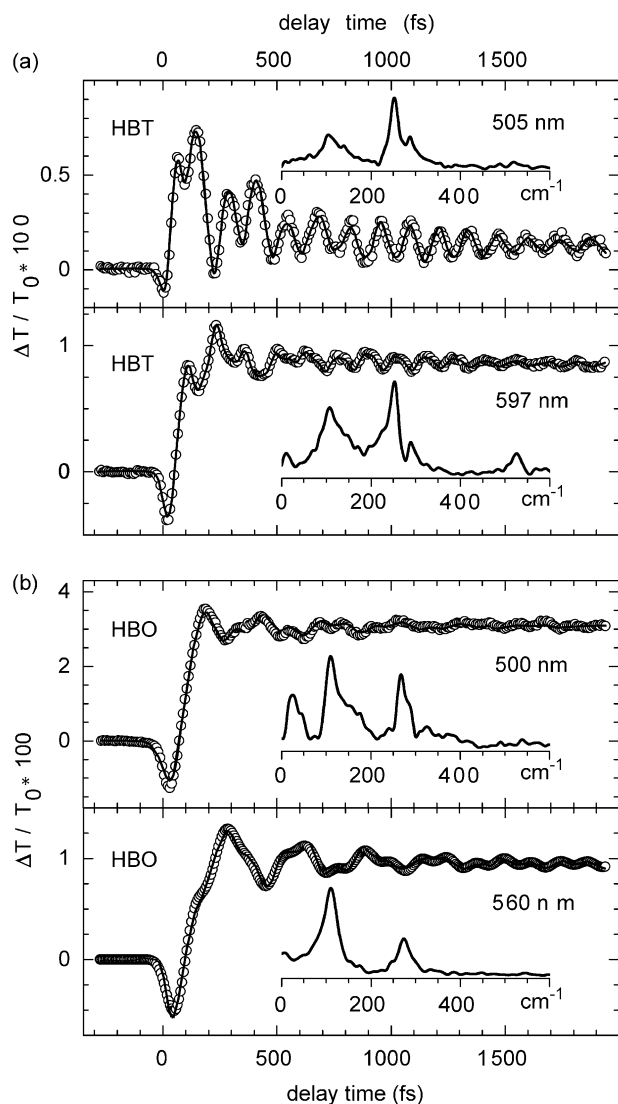


Fig. 1. (a) Time resolved transmission change due to excitation of HBT at 347 nm probed at 505 and 597 nm. (b) Transient transmission of HBO excited at 340 nm and probed at 500 and 560 nm. The data (open circles) are depicted together with the results of the fitting procedure (solid lines). The insets show the Fourier transforms of the oscillatory signal components.

contributions are fitted by exponentially damped cosine functions. The frequencies of the dominant contributions are listed in Table 1. The damping times are found to be on the order of 500 fs [8,10]. This is in excellent agreement with vibrational redistribution times of about 700 fs found by time resolved IR spectroscopy [18].

The rise of emission indicates the delay time when the molecule reaches the area of the PES belonging to the product state. Since the emission rise can be modeled by a delayed step instead of an exponential change and because the molecules show coherently excited vibrational motions after the ESIPT, we conclude that the whole process evolves as a ballistic wavepacket motion [8,10,15]. The wavepacket launched by the pump pulse at the Franck–Condon point

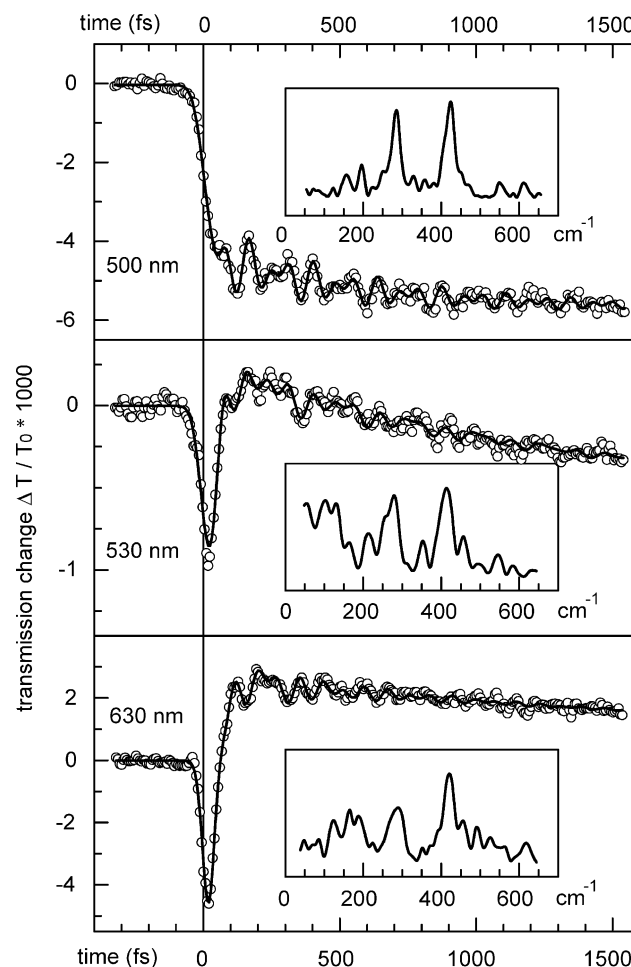


Fig. 2. Time resolved transmission change (open circles) for OHBA excited at 340 nm probed at 500, 530, and 630 nm together with the fitted model functions (solid lines). The Fourier transforms of the oscillatory contributions are depicted in the insets.

follows a path on the S_1 PES that is governed by the steepest descent. It stays quite confined and no splitting or strong spreading is observed. According to the Ehrenfest theorem the center of gravity of the wavepacket moves in an almost classical fashion [19]. This allows us to describe the process by a model with classical features. Furthermore, these

Table 1
Fit results for the emission delay and the two dominant frequencies

Compound	Wavelength (nm)	Delay (fs)	First frequency (cm^{-1})	Second frequency (cm^{-1})
HBT	505	39	113	254
	597	52	106	256
HBO	500	90	114	273
	560	80	110	271
OHBA	500	41	285	427
	530	44	275	419
	630	46	296	420

observations indicate that no significant energy barrier is encountered along the reaction path.

The emission rise indicates the arrival of the wavepacket in the keto region of the PES. Its delay is a measure for the duration of the ESIPT. In the case of HBT and OHBA, the observed delays are on the order of 40–50 fs (see Table 1) [8,10]. The delays observed for HBO are 80–90 fs and quite similar to the exponential time constants found in previous studies [9,20,21]. They are significantly longer than those of HBT and OHBA. We think that in the case of HBO the initial acceleration in the Franck–Condon region is weaker than in the other two molecules. However, in all cases, the delay is on the sub-100 fs time-scale. It is, however, still too long for a barrierless motion of only the proton [12]. This indicates that skeletal deformations determine the duration of the process and the inertia of the contributing nuclei is responsible for the surprisingly large delay.

The similarities in the observed dynamics of HBT, HBO and OHBA are striking. Measurements on the significantly larger ESIPT compound *N,N'*-bis(salicylidene)-*p*-phenylenediamine reveal again a transfer time of about 50 fs [22] and the coherent wavepacket dynamics observed in the case of TINUVIN P [13] has very similar features compared to the molecules investigated in this study. This similarity exists even so the excited state lifetime of TINUVIN P is only 120 fs and thereby 100–1000 times shorter than for the other compounds [17]. Recently, time resolved ionization measurements also found a coherent wavepacket motion associated with the ESIPT of *o*-hydroxyacetophenone [23]. From these similarities, we conclude that fine variations in the electronic structure are not important for the dynamics. This is especially supported by the results on OHBA where an oxygen atom is the proton acceptor whereas most of the other compounds have a nitrogen atom at this position.

3.2. Skeletal motions during the transfer

The coherent excitation of vibrational modes has its origin in the molecular motion along specific coordinates during the ESIPT [8,24]. In the process, the molecule follows a curved reaction path in the multi-dimensional space spanned by the nuclear degrees of freedom. A small number of vibrational coordinates contributes significantly to the reaction and only for these modes the distortion of the molecule along the reaction path has large projections. When the molecule arrives at the product minimum, it has momentum along the same coordinates. This causes coherent vibrational motions in modes that correspond to these coordinates. The identification of the coherently excited modes reveals the coordinates contributing to the reaction path. This can be accomplished by comparing the oscillation frequencies observed in the experiments with calculated vibrational normal modes. We restrict ourselves in most cases to density functional theory calculations in the electronic ground state because ab initio calculations in the excited state are very challenging and the low frequency

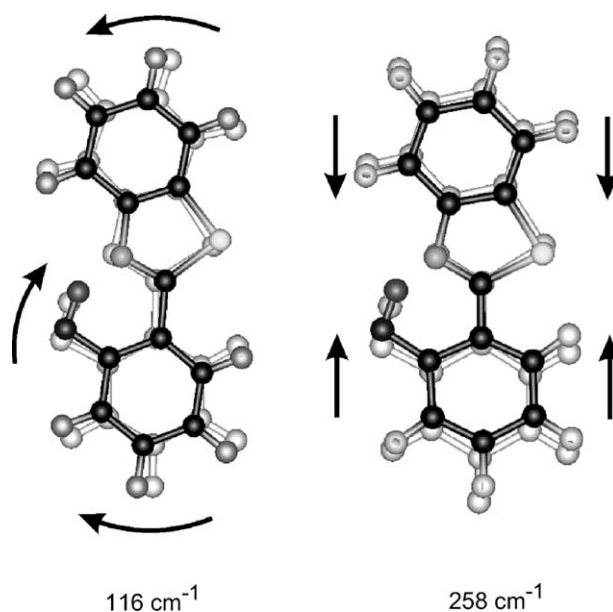


Fig. 3. Calculated vibrational eigenmodes and frequencies of HBT that correspond to the dominant oscillatory signal contributions.

normal modes are found to be very similar in both states. This is indicated by the good agreement between the calculated and observed frequencies and was confirmed by high level ab initio calculations on HBT [24].

In Fig. 3, the two vibrational eigenmodes are depicted that dominate the oscillatory signal contributions in HBT and HBO. The calculated vibrational frequencies of HBT are given in Fig. 3 and coincide almost perfectly with the observed frequencies listed in Table 1. In the case of HBT, we demonstrated that in total four modes are coherently excited, but the contribution of the two modes not shown here is much smaller [8,15]. In HBT and HBO, the same modes are coherently excited showing that their reaction paths are very similar. Both modes lead to in-plane deformations of the H-chelate ring and especially to the variation of the distance between the hydrogen donating oxygen atom and the accepting nitrogen atom. Several other vibrational modes exist with frequencies in the observable range up to 600 cm^{-1} . But they are not or only very weakly coherently excited indicating that they represent deformations that are of minor relevance for the ESIPT process.

Fig. 4 shows the normal modes that give rise to the oscillatory signal contributions in the case of OHBA. Both modes lead again to in-plane deformations of the H-chelate ring. The mode calculated at 274 cm^{-1} and observed around 285 cm^{-1} (compare Fig. 4 and Table 1) is a bending motion of the carbonyl group and a counter rotation of the rest of the molecule to conserve angular momentum. The 420 cm^{-1} mode changes the in-plane angles of the entire molecular skeleton. In the case of HBT and HBO the two dominant modes lead to a bending or a contraction of the whole molecular skeleton whereas the 285 cm^{-1} mode of OHBA is an almost local bending of the carbonyl group.

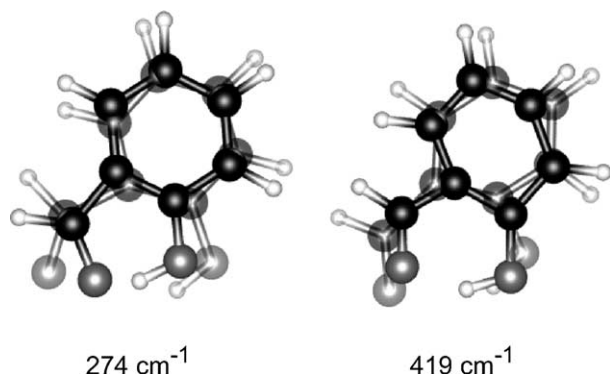


Fig. 4. Calculated vibrational eigenmodes and frequencies of OHBA that correspond to the dominant oscillatory signal contributions.

However, all these motions have in common that they vary very efficiently the donor–acceptor distance. Even the OHBA mode at 420 cm^{-1} influences significantly this distance (see Fig. 4).

Because the donor–acceptor distance is changed by each coherently excited vibrational mode in all three molecules we conclude that during the PT it adapts values that differ strongly from the equilibrium geometry of both the enol and the keto form. It has to be drastically reduced before the proton can be bonded to the acceptor atom. In the case of HBT, we found indications that the bending of the molecular skeleton is the dominant initial motion and leads indeed directly to a shortening of the donor–acceptor distance [8]. Because the coherently excited vibrations likewise affect in-plane angles and bond lengths of the H-chelate ring these parameters seem to experience also a readjustment during the ESIPT. The ab initio calculations totally confirm this picture derived from the experimental observations and find a decrease of the donor–acceptor distance of up to 0.3 \AA along the minimum energy path from the Franck–Condon point to the keto minimum [24].

From these findings, the following picture of the nuclear motions during the transfer emerges [8,10,24]. After the molecule is promoted by the optical excitation to the Franck–Condon point, it performs a bending motion that reduces the donor–acceptor distance. When the hydrogen atom is shifted together with the oxygen atom sufficiently near to the acceptor atom a change of the electronic wave function is possible without the need of extra energy or a tunneling process through a barrier. The new electronic wave function is associated with the formation of a new bond between the hydrogen and the acceptor atom and the change of the strength of other bonds. A new equilibrium geometry is associated with the new bonds and the molecular skeleton performs motions in order to adjust to this geometry. Thereby the wavepacket evolves also along other coordinates that are strongly coupled to the donor–acceptor distance. When the molecule geometry arrives at the keto minimum of the excited state PES, it does

not stop its evolution but propagates further according to the nuclear momenta. This ringing of the molecule corresponds to the damped oscillatory motions around the keto minimum that are observed in the experimental signal.

3.3. Electronic configuration change and adiabatic evolution

Time resolved IR experiments show for HBT that after UV excitation the C=O stretch vibration appears on a time-scale of $30\text{--}50\text{ fs}$ [25]. This demonstrates that in the course of the ESIPT the H-donor bond is indeed broken and new bonds are formed. The occupation of the electronic orbitals changes during the process and the electronically excited enol form has a different electronic configuration as the resulting S_1 keto form. However, the observation of a well-defined wavepacket after the transfer indicates that the change of the electronic configuration is not associated with a jump between two energetically separated electronic states. Rather we describe the PT as an evolution on a single adiabatic PES. During the evolution, the wave function changes its electronic character. To discuss the properties of the adiabatic PES we start out with the two diabatic surfaces belonging to the enol and the keto configuration that would be the relevant surfaces if the electronic configurations would not mix. In the case of strong coupling two adiabatic surfaces emerge from the mixing of the two diabatic PESs and the reaction path follows the energetically lower one [26]. The path involves several molecular coordinates that contribute with varying magnitude resulting in changes of the path direction in coordinate space. The initial acceleration in the Franck–Condon region points toward the minimum of the diabatic PES of the S_1 -enol configuration as was demonstrated for HBT by ab initio calculations [24]. However, the enol and the keto configuration couple very strongly with each other. This leads to an efficient mixing of both configurations and to a strong deformation of the resulting adiabatic PES with respect to the original diabatic PESs. In the region of the diabatic enol minimum, the adiabatic PES has a slope toward the region with increasing configuration mixing. The mixing is most efficient where the two diabatic PESs intersect. The change of the electronic configuration takes place when the wavepacket propagates through this part of the adiabatic PES. Thereafter, the slope of the PES is directed toward the keto minimum. Because of the strong coupling between both configurations a barrierless or almost barrierless reaction path results. From the coupling of the two diabatic PESs a second adiabatic PES at higher energies is expected. However, it will be difficult to locate this state in the dense manifold of higher electronically excited states.

Reliable ab initio calculations dealing with the ESIPT mechanism are very complex and challenging [24,27]. The reason is that the shape of the PES is determined by two electronically excited configurations and the coupling between them. It is necessary to use an accurate description

of the electronic configurations and to account for electron correlation effects [27]. However, such calculations were recently performed for HBT and find in nice agreement with our experimental results that a contraction of the donor–acceptor distance is needed to transfer the proton and that this contraction seems to result from skeletal motions [24].

The propagation of the wavepacket along the reaction path is first of all associated with skeletal motions of the molecule (see above). The proton is initially shifted together with the oxygen atom and after the configuration change together with the acceptor atom. It stays all the time in or nearby the minimum of its local potential well that is moved by the skeletal motions. Several findings support this point of view. If the ES IPT would mainly be the direct motion of the proton from the donor site to the acceptor site it should be much faster because of the small proton mass [12] or it must be hindered by a barrier. Tunneling through the barrier as well as thermally activated crossing over the barrier should not lead to a ballistic wavepacket motion of the whole system as observed. Furthermore, if the proton would not stay at its local minimum an excitation of its local vibrational mode should occur. However, the excitation of such high frequency modes seems to be highly unlikely according to IR experiments [18,25] and energy considerations [8].

4. Conclusions

Transient absorption measurements with 30 fs time resolution are able to reveal the nuclear motions during an ultrafast reactive process via the ringing of the molecule in coordinates that contribute to the reaction path. These periodic nuclear motions persist long after the actual process itself is finished within less than 100 fs. The ES IPT processes of HBT, HBO and OHBA are investigated in real time and strong similarities in the dynamics are observed. By comparing the results, we find a common mechanism. After optical excitation with an ultrashort pulse, the created wavepacket propagates in a ballistic fashion along the adiabatic PES of the S_1 state. The wavepacket propagation is associated with a bending motion of the molecular skeleton that reduces the proton donor–acceptor distance. An electronic configuration change occurs at a sufficient contraction and leads to the bonds of the product conformer. The shape of the PES is determined by the coupling between the electronic enol and keto configuration and the generation of the new bonds can be described as the mixing of both configurations during the wave packet propagation. The proton itself stays at its local potential minimum that is shifted with the motions of the molecular skeleton.

Acknowledgements

We are indebted to Alexander J. Wurzer, Tanja Bizjak, Regina de Vivie-Riedle, and Vincent De Waele for valuable contributions and discussions and gratefully acknowledge funding by the Deutsche Forschungsgemeinschaft.

References

- [1] T. Bountis (Eds.), *Proton Transfer in Hydrogen-Bonded Systems*, Plenum Press, New York, 1992.
- [2] P.F. Barbara, H.P. Trommsdorff (Eds.), *Special Issue on Spectroscopy and Dynamics of Elementary Proton Transfer in Polyatomic Systems*, *Chem. Phys.* 136 (1989) 153–360.
- [3] A. Douhal, F. Lahmani, A. Zehnacker-Rentien, *Chem. Phys.* 178 (1993) 493.
- [4] H.-H. Limbach, J. Manz (Eds.), *Special Issue on Hydrogen Transfer: Experiment and Theory*, *Ber. Bunsenges. Phys. Chem.* 102 (1998) 289–592.
- [5] A.H. Zewail, *J. Phys. Chem. A* 104 (2000) 5660.
- [6] A. Weller, *Z. Elektrochem.* 60 (1956) 1144.
- [7] F. Laermer, T. Elsaesser, W. Kaiser, *Chem. Phys. Lett.* 148 (1988) 119.
- [8] S. Lochbrunner, A.J. Wurzer, E. Riedle, *J. Phys. Chem. A* 107 (2003) 10580.
- [9] T. Arthen-Engeland, T. Bultmann, N.P. Ernsting, M.A. Rodriguez, W. Thiel, *Chem. Phys.* 163 (1992) 43.
- [10] K. Stock, T. Bizjak, S. Lochbrunner, *Chem. Phys. Lett.* 354 (2002) 409.
- [11] P.F. Barbara, L.E. Brus, P.M. Rentzepis, *J. Am. Chem. Soc.* 102 (1980) 5631.
- [12] J.L. Herek, S. Pedersen, L. Bañares, A.H. Zewail, *J. Chem. Phys.* 97 (1992) 9046.
- [13] C. Chudoba, E. Riedle, M. Pfeiffer, T. Elsaesser, *Chem. Phys. Lett.* 263 (1996) 622.
- [14] A.J. Wurzer, S. Lochbrunner, E. Riedle, *Appl. Phys. B* 71 (2000) 405.
- [15] S. Lochbrunner, A.J. Wurzer, E. Riedle, *J. Chem. Phys.* 112 (2000) 10699.
- [16] E. Riedle, M. Beutter, S. Lochbrunner, J. Piel, S. Schenkl, S. Spörlein, W. Zinth, *Appl. Phys. B* 71 (2000) 457.
- [17] S. Lochbrunner, E. Riedle, *Recent Res. Dev. Chem. Phys.* 4 (2003) 31.
- [18] M. Rini, J. Dreyer, E.T.J. Nibbering, T. Elsaesser, *Chem. Phys. Lett.* 374 (2003) 13.
- [19] C. Cohen-Tannoudji, B. Diu, F. Laloe, *Quantum Mechanics*, vol. 1, Wiley-Interscience, New York, 1977, p. 242.
- [20] O.K. Abou-Zied, R. Jimenez, E.H.Z. Thompson, D.P. Millar, F.E. Romesberg, *J. Phys. Chem. A* 106 (2002) 3665.
- [21] H. Wang, H. Zhang, O.K. Abou-Zied, C. Yu, F.E. Romesberg, M. Glasbeek, *Chem. Phys. Lett.* 367 (2003) 599.
- [22] M. Ziótek, J. Kubicki, A. Maciejewski, R. Naskrecki, A. Grabowska, *Chem. Phys. Lett.* 369 (2003) 80.
- [23] C. Su, J.-Y. Lin, R.-M.R. Hsieh, P.-Y. Cheng, *J. Phys. Chem. A* 106 (2002) 11997.
- [24] R. de Vivie-Riedle, V. De Waele, L. Kurtz, E. Riedle, *J. Phys. Chem. A*, 107 (2003) 10591.
- [25] M. Rini, A. Kummrow, J. Dreyer, E.T.J. Nibbering, T. Elsaesser, *Faraday Discuss.* 122 (2002) 27.
- [26] M. Klessinger, J. Michl, *Excited States and Photochemistry of Organic Molecules*, VCH Publishers, New York, 1995, p. 182.
- [27] A.L. Sobolewski, W. Domcke, *Phys. Chem. Chem. Phys.* 1 (1999) 3065.